

Improvements in Spatial and Color Adaptive Gamut Mapping Algorithms

Nicolas Bonnier^{*,**}, Christophe Leynadier^{*} and Francis Schmitt^{**}

^{*} Océ Print Logic Technologies, Créteil, France.

^{**} Institut TELECOM, TELECOM ParisTech, LTCI CNRS, France.

nicolas.bonnier@oce.com, christophe.leynadier@oce.com, francis.schmitt@telecom-paristech.fr

Abstract

Two spatial and color adaptive gamut mapping algorithms have recently been introduced. We propose and evaluate a set of modifications to improve their results. Modifications include a change in the image decomposition in two bands with an initial Black Point Compensation (BPC) applied to the low-pass band followed by an adaptive merging of the two bands.

Introduction

In the quest for an optimal reproduction of a color image, an impressive number of Gamut Mapping Algorithms (GMAs) have been proposed in the literature. Morovic and Luo have made an exhaustive survey in [1]. After much efforts to improve adaptive GMAs, it has been advocated that preservation of the spatial details in an image is a very important issue for perceptual quality [2, 3]. GMAs adaptive to the spatial content of the image, i.e. Spatial Gamut Mapping Algorithms (SGMAs), have been introduced. These new algorithms try to balance both color accuracy and preservation of details, by acting locally to generate a reproduction perceived as close to the original. "One of the fundamental motivations of spatial gamut mapping is the need to preserve the edge between two out-of-gamut colors, which would otherwise map individually to the same in-gamut color" [4]. There are a limited number of publications regarding this recent and important development. Meyer and Barth [5] first introduced a SGMA, followed by Kasson [6] Nakauchi et al. [7], XSGM by Bala et al. [8], McCann [2], MSGM4 by Morovic and Wang [9], Kimmel et al. [4], Zolliker et al. [10] and Farup et al. [11]. We distinguish two groups of SGMAs which follow different approaches: the first one called *compensation approach* reinserts high-frequency content in clipped images to compensate for the loss of details caused by clipping, the second one called *optimization approach* uses iterative optimization tools.

Two new *Spatial and Color Adaptive Gamut Mapping Algorithms* (SCAGMAs) have been recently introduced in [12], *Spatial and Color Adaptive Compression* (SCACOMP) and *Spatial and Color Adaptive Clipping* (SCACLIP). Based on spatial color bilateral filtering, they both take into account the color properties of the neighborhood of each pixel. Their goal is to preserve both the color values of the pixels and their relations between neighbors. While psycho-physical experiments have validated SCACOMP and SCACLIP, they show that results for certain categories of images are not optimal. Our aim is to propose a set of modifications of the algorithms to improve these results.

SCACOMP and SCACLIP

These two adaptive algorithms are described by the diagram in Fig. 1 and by the following process:

1. Conversion of the original image to the CIELAB color space using the relative colorimetric intent of the input ICC

profile: \mathbf{I}_{in} .

2. Decomposition in low-pass and high-pass bands using bilateral filtering (BF) [13]: \mathbf{I}_{low} and \mathbf{I}_{high} .
3. *HPMinΔE* clipping [14] of the low-pass band: \mathbf{I}_{low}^- .
4. Merging of \mathbf{I}_{low}^- and \mathbf{I}_{high} .
5. Adaptive mapping: \mathbf{I}_{out} .
6. Conversion to the CMYK encoding of the output printer using the relative colorimetric intent of its ICC profile.

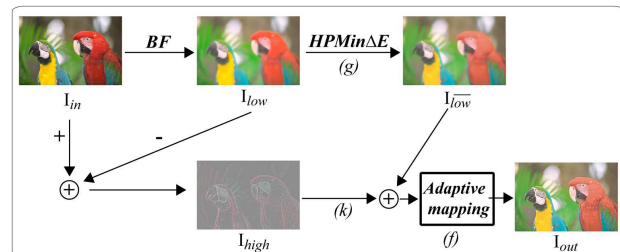


Figure 1. Framework for SCACOMP and SCACLIP.

SCACOMP and SCACLIP only differ in step 5:

- SCACOMP proposes an adaptive compression algorithm to preserve the color variations between neighboring pixels contained by \mathbf{I}_{high} . The concept is to project each color of pixel lying outside the destination gamut $Gamut_{Dest}$ toward the 50% greypoint of $Gamut_{Dest}$ [15], more or less deeply inside the gamut depending on its neighbors (see Fig. 5).
- SCACLIP proposes to set the direction of the projection as a variable: for each pixel the optimal mapping direction will be chosen so that the local variations are best maintained according to a local energy criterion (see Fig. 6).

Drawbacks

When considering the proposed algorithms and after analyzing the resulting images they produce, we observe the following:

- Results of both SCAGMAs on colorful images are very good, i.e. color attributes and details are well preserved, except for a few images where artifacts from the initial gamut mapping *HPMinΔE* on \mathbf{I}_{low} are noticeable.
- Results on low-key images are average, the darkest regions appearing to be noisy. In our experimental setup, the values of the black points of the input and destination gamuts was $L^* = 0$ and $L^* = 27$ respectively. Thus large parts of low-key images have been clipped by the initial *HPMinΔE* of \mathbf{I}_{low} . When high-pass content \mathbf{I}_{high} is added to the severely altered \mathbf{I}_{low}^- , the resulting images appears unnatural.
- Details in resulting images look significantly better when displayed on a monitor, but improvement is not as much striking on prints.

Modifications in the workflow

Based on these observations, we are now investigating a set of modifications in the proposed color re-rendering workflow aimed at enhancing the final results. In the following sections, modifications are proposed for several steps of the process, including the image decomposition, an initial Black Point Compensation (BPC) algorithm applied to the low-pass band, an adaptive merging of the two bands, and evolutions of the spatial and color adaptive gamut mapping algorithms. The diminution of details caused by the modulation transfer function of the printing process is currently being investigated [?].

Image decomposition

One key aspect of the proposed SCAGMAs is the decomposition of the image in two bands (see Fig. 1). The goal of this decomposition is to set apart the local means and the local details of the image in order to process them separately and preserve both as much as possible in the resulting image. In classic gaussian filtering, the width of the gaussian (set by σ_d) determines the boundary between the ‘lower’ frequency content going to the low-pass band (considered as local means) and the ‘higher’ frequency content going to the high-pass band (local details). Setting the appropriate value for σ_d is not a trivial task. This choice relates to the definition of ‘local details’ (i.e. small or minor elements in a particular area). This definition depends on multiples parameters such as the size and resolution of the reproduction, the modulation transfer function of the reproduction device, the viewing conditions, the distance of visualization and the behavior of the human visual system. The human visual system is often modeled by multi-scale decompositions [16] with more than two bands (usually up to five). Such multi-scale decomposition has been proposed in the spatial gamut mapping MSGM by Morovic and Wang [9]. It could be relevant in our algorithm and would allow the definition of several categories of details with different sizes. However for the sake of keeping the algorithm simple and the computing cost low, we limit the image decomposition to two bands. Thus we need to investigate the impact of σ_d on the decomposition to select an appropriate value.

Furthermore, to avoid the introduction of halos [12] the decomposition in SCACLIP and SCACOMP is obtained by 5D Bilateral Filtering (BF) in the CIELAB space as proposed by Tomasi and Manduchi in [13]. It is a combined spatial domain and color range filtering. Let $L_{BF} = BF(L)$, $a_{BF} = BF(a)$, $b_{BF} = BF(b)$ denote the three channels of the filtered image. The L_{BF} value of pixel i , L_{BF}^i , can be obtained as follows (similar expressions for a_{BF}^i and b_{BF}^i):

$$L_{BF}^i = \sum_{j \in \mathbf{I}_{in}} w_{BF}^j L^j, \quad (1)$$

$$w_{BF}^j = \frac{d(\mathbf{x}^i, \mathbf{x}^j) r(\mathbf{p}^i, \mathbf{p}^j)}{\sum_{j \in \mathbf{I}_{in}} d(\mathbf{x}^i, \mathbf{x}^j) r(\mathbf{p}^i, \mathbf{p}^j)}, \quad (2)$$

where \mathbf{I}_{in} is the original image, $d(\mathbf{x}^i, \mathbf{x}^j)$ measures the geometric closeness between the locations \mathbf{x}^i of pixel i and \mathbf{x}^j of a nearby pixel j . $r(\mathbf{p}^i, \mathbf{p}^j)$ measures the colorimetric similarity between the colors (L^i, a^i, b^i) and (L^j, a^j, b^j) of pixels i and j . In our implementation, $d(\mathbf{x}^i, \mathbf{x}^j)$ and $r(\mathbf{p}^i, \mathbf{p}^j)$ are gaussian functions of the euclidean distance between their arguments:

$$d(\mathbf{x}^i, \mathbf{x}^j) = e^{-\frac{1}{2} \left(\frac{\|\mathbf{x}^i - \mathbf{x}^j\|}{\sigma_d} \right)^2}, \quad r(\mathbf{p}^i, \mathbf{p}^j) = e^{-\frac{1}{2} \left(\frac{\Delta E_{ab}(\mathbf{p}^i, \mathbf{p}^j)}{\sigma_r} \right)^2}. \quad (3)$$

where the two scale parameters σ_d and σ_r play an essential role in the behavior of the filter.

In the 5D bilateral filter the ΔE_{ab} color distance between the central pixel and nearby pixels is taken into account. This allows us to avoid halos and to handle specifically the local transitions between local similar pixels. Nearby pixels at small ΔE_{ab} distance (i.e. perceived as similar) are filtered. Pixels are less and less filtered as the ΔE_{ab} distance becomes large compared to σ_r . Thus σ_r determines a reference to set apart small ΔE_{ab} from large ΔE_{ab} . While small ΔE_{ab} values are well correlated with perceived color differences, it is more difficult to define a threshold σ_r above which ΔE_{ab} values can be considered as large. One goal of the SCAGMAs is to preserve colors that would be mapped by gamut mapping algorithms to the same color of the destination gamut. Thus to set σ_r , the average distance between the input and destination gamuts might be considered. The ability of the output device to maintain small differences between colors could also be taken into account [?].

Given the lack of a straightforward definition for ‘local details’ and ‘similar colors’, we propose to review the previous work and to evaluate the impact of σ_d and σ_r values on the image decomposition.

Previous work

Tomasi and Manduchi [13] explore different values for σ_d and σ_r , and present 8 bits grayscale images processed with $\sigma_d = 3$ pixels and $\sigma_r = 50$, yet the sizes of the processed images are not specified. As the setting of σ_d should depend on the image size and the conditions of visualization, Zolliker and Simon [10] obtained good results with σ_d in the range of [2,5]% of the image diagonal and σ_r values in the range of [10,25] ΔE_{ab} . They have applied the filter in their spatial gamut mapping algorithm with $\sigma_d = 4\%$ of the image diagonal and $\sigma_r = 20\Delta E_{ab}$.

In the first implementation of SCACLIP and SCACOMP we empirically set the values to $\sigma_d = 1\%$ of the image diagonal and $\sigma_r = 25\Delta E_{ab}$ (for images printed at 150 dpi, at the size [9-15] cm by [12 - 20] cm, viewed at a distance of 60 cm). This value $\sigma_d = 1\%$ of the image diagonal is not in the range proposed by Zolliker and Simon but the context and the filtered images are different: they filter image differences and we filter the whole image. This mean that the characteristics (contrast, saturation...) are different and the settings of the bilateral filter may consequently differ.

Experiment

In the following we investigate the impact of the value of σ_d and σ_r on the image decomposition. Each parameter is set at different values: $\sigma_r = 5, 10, 20, 40, 80 \Delta E_{ab}$ and $\sigma_d = 5, 10, 20, 40, 80$ pixels, i.e. for an image size of 1125 x 750: $\sigma_d = 0.37, 0.74, 1.49, 2.99, 5.98 \%$ of the diagonal of the image. In SCACLIP and SCACOMP, 5D Bilateral Filter is applied to the lightness and the chroma: the original CIELAB image is first converted to the polar representation CIELCH, i.e. Lightness, chroma and hue. To compute the low-pass band \mathbf{I}_{low} , only the two channels L_{in} and c_{in} of the original image \mathbf{I}_{in} are filtered using 5D bilateral filtering as described above (Eq.1-3). The h_{in} channel is not filtered, to keep the hue unaltered. Nevertheless, since the 5D bilateral filter involves ΔE_{ab} distance, the hue is taken into account in the filtering of L_{in} and c_{in} channels. The high-pass band \mathbf{I}_{high} is then calculated by taking the difference of \mathbf{I}_{in} and the low-pass band \mathbf{I}_{low} :

$$\mathbf{I}_{low} = (L_{BF}, c_{BF}, h_{in}), \quad (4)$$

$$\mathbf{I}_{high} = \mathbf{I}_{in} - \mathbf{I}_{low} = (L_{in} - L_{BF}, c_{in} - c_{BF}, 0), \quad (5)$$

where $L_{BF} = BF(L_{in})$ and $c_{BF} = BF(c_{in})$.



Figure 2. Impact of the values of σ_d and σ_r on \mathbf{I}_{low} . Left to right: $\sigma_r = 5, 10, 20, 40, 80 \Delta E_{ab}$, top to bottom: $\sigma_d = 5, 10, 20, 40, 80$ pixels.

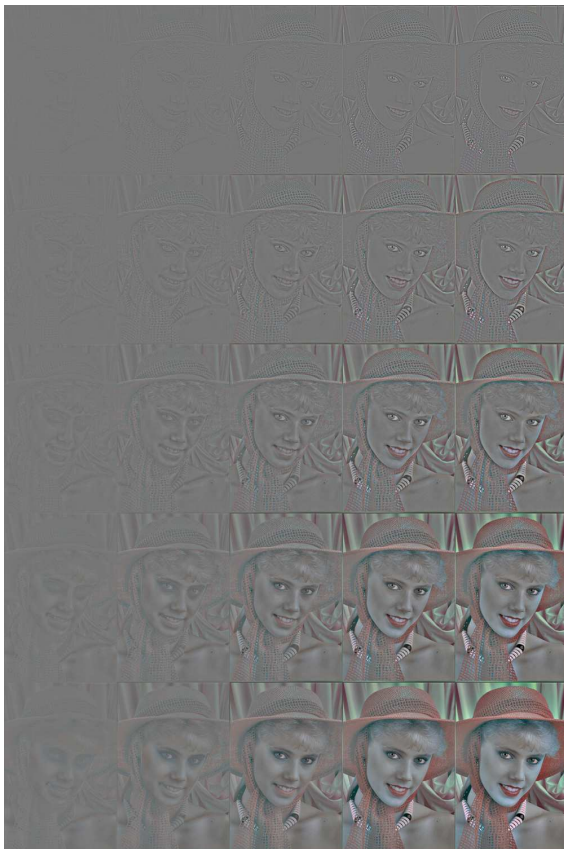


Figure 3. Impact of the values of σ_d and σ_r on \mathbf{I}_{high} . Left to right: $\sigma_r = 5, 10, 20, 40, 80 \Delta E_{ab}$, top to bottom: $\sigma_d = 5, 10, 20, 40, 80$ pixels. A constant $[50,0,0]$ was added to the CIE Lab values for illustration purpose.

In Figures 2 and 3 we observe the impact of varying the values of σ_d and σ_r on \mathbf{I}_{low} and \mathbf{I}_{high} respectively. From the top to the bottom: $\sigma_d = 5, 10, 20, 40, 80$ pixels and from left to right $\sigma_r = 5, 10, 20, 40, 80 \Delta E_{ab}$.

Analysis

A larger value of σ_d means a broader filter in the image domain, thus a larger set of frequencies being filtered. Indeed in Figures 2 and 3, when browsing the mosaic of images from top to bottom, one observes that \mathbf{I}_{low} becomes blurrier and \mathbf{I}_{high} presents more and more details.

A larger value of σ_r means a larger filter in the color domain, thus a larger range of color transitions being filtered. When σ_r is very large, the bilateral filter is not modulated by the color content of the filtered area and the resulting blurring of the image is similar to the blurring of a two dimensional gaussian filter. It also leads to the introduction of halos near the strong edges. In Figure 3, when browsing the image from left to right, one finds more and more color content in \mathbf{I}_{high} .

We now consider the relation between σ_d and σ_r . A small value of σ_r severely limits the blurring of the image to very small color transitions for any σ_d . A small value of σ_d limits the blurring of the image to high frequency content for any σ_r . When both σ have very large values, \mathbf{I}_{low} shows some color shifts due to a large boost of chroma in desaturated areas surrounded by saturated areas. These would cause trouble in the gamut mapping process, yet it only occurs for very large σ values.

Selection of σ_d and σ_r

Based on our observations, we find that values $\sigma_r = 20 \Delta E_{ab}$ and $\sigma_d = 20$ pixels (i.e. approximately 1.5% of the diagonal) to be a good compromise which suits these algorithms and our set of images. Further studies remains necessary to set these parameters with more objective methods.

Black Point Compensation of \mathbf{I}_{low}

Scaling the dynamic range of the image to fit in the output dynamic range is often part of rendering workflows. Applied before the gamut mapping algorithm, it avoids consequent clipping of low-key values in the image. In the following section we discuss several scaling options found in the literature, select an algorithm and include it in the workflow of the SCAGMAs.

Choice of color space

Black Point Compensation (BPC) [17] also referred to as linear XYZ scaling [18] maps the source's black point to the destination's black point in the CIEXYZ color space, hence scaling intermediate color values. Alternatively a Lightness Compression Algorithm (LCA) also named lightness scaling, rescaling or remapping might be applied to the image in the CIELAB color space. Linear, polynomial and sigmoidal LCAs [19, 20] have been proposed and implemented in point-wise (i.e. non spatial) color workflows. Experimental results [19, 20] suggest that the performance of sigmoidal scaling depends on the magnitude of gamut difference and might be image-dependent. XYZ scaling is considered by Holm in [18] as a baseline color re-rendering for reasonably similar output-referred source and destination media. Most point-wise ICC [21] workflow implementations apply linear CIEXYZ scaling (e.g. Adobe in [17]).

Lightness scaling is also proposed in existing spatial gamut mapping algorithms: Meyer and Barth propose to apply a linear compression to the low spatial-frequency band in the log domain [5]. In MSGM by Morovic and Wang [9], an optional sigmoidal

lightness compression of the J channel in CIECAM97 space low-est spatial-frequency band is proposed. Similar techniques have also been used to render High Dynamic Range (HDR) images, such as in Durand and Dorsey [22] where the range of the base layer is compressed using a scale factor in the log domain of the rgb pixel values.

Black Point Compensation and Gamut Mapping

While SCACLIP and SCACOMP proposed in [12] did not include BPC, such algorithm improves the quality of the results. In our workflow we now apply linear image dependent CIE XYZ scaling where the low spatial-frequency band I_{low} is first converted to a normalized flat XYZ encoding with white point = [1,1,1] and its range scaled to fit into the range of the destination device as proposed in [17]. The Y_{lowBPC} value of pixel i , Y_{lowBPC}^i , is obtained as follows (similar expressions for X_{lowBPC}^i and Z_{lowBPC}^i):

$$Y_{lowBPC}^i = \frac{Y_{low}^i - Y_{minlow}}{1 - Y_{minlow}}(1 - Y_{minDest}) + Y_{minDest}, \quad (6)$$

where Y_{lowBPC}^i is the scaled Y value of the destination pixel i , Y_{low}^i the Y value of the source pixel i , Y_{minlow} the minimum Y value of the image and $Y_{minDest}$ the minimum Y value of the destination device. The resulting image is then converted to CIELCH. In

Legend of Figure 4. Impact of black point compensation.

No BPC	BPC
I_{low}	I_{lowBPC}
$I_{low}^{\overline{}}$	$I_{lowBPC}^{\overline{}}$
Out-of-gamut pixels in I_{low}	Out-of-gamut pixels in I_{lowBPC}
Distance to gamut in I_{low}	Distance to gamut in I_{lowBPC}

Fig. 4 we compare two scenarios: the left column shows the process without Black Point Compensation, and the right column the process with BPC. Top row I_{low} (left) is compared with I_{lowBPC} (right). In second row gamut mapped: $I_{low}^{\overline{}}$ (left) is compared with BPC and gamut mapped $I_{lowBPC}^{\overline{}}$ (right). Notice the artifacts in $I_{low}^{\overline{}}$ (i.e. the color shifts in the strawberries). In third row a light cyan mask of the out of gamut pixels in I_{low} (left) and I_{lowBPC} (right). Bottom row: representation of the distance to gamut of out of gamut pixels in I_{low} (left) and I_{lowBPC} (right). Constant [50,0,0] grey was added to the difference CIELAB image for illustration purpose. BPC significantly decrease the number of out of gamut pixels and the distance between the gamut and these pixels. Notice that Black Point Compensation can be considered as a gamut compression algorithm. As such, it produces images that are less saturated (see first row of Fig. 4). This desaturation is not always welcomed and/or necessary. Thus we propose to apply BPC on an image basis only if large parts of the image are significantly below the level of the output black point and we will investigate this possibility in future experiments.

Since the BPC in CIE XYZ scales down the gamut of I_{low} , boundaries of I_{lowBPC} 's gamut are closer to the destination gamut and the choice of initial clipping has less impact on the final results. In previous experiments [12] some colorful images clipping artifacts were noticeable. These artefacts were due to the initial clipping using $HPMin\Delta E_{ab}$. However such artifacts are no longer an issue when applying the black point compensation first (see second row of Fig. 4). And $HPMin\Delta E_{ab}$ is appropriate to preserve the saturation:

$$I_{low}^{\overline{}} = HPMin\Delta E(I_{lowBPC}). \quad (7)$$

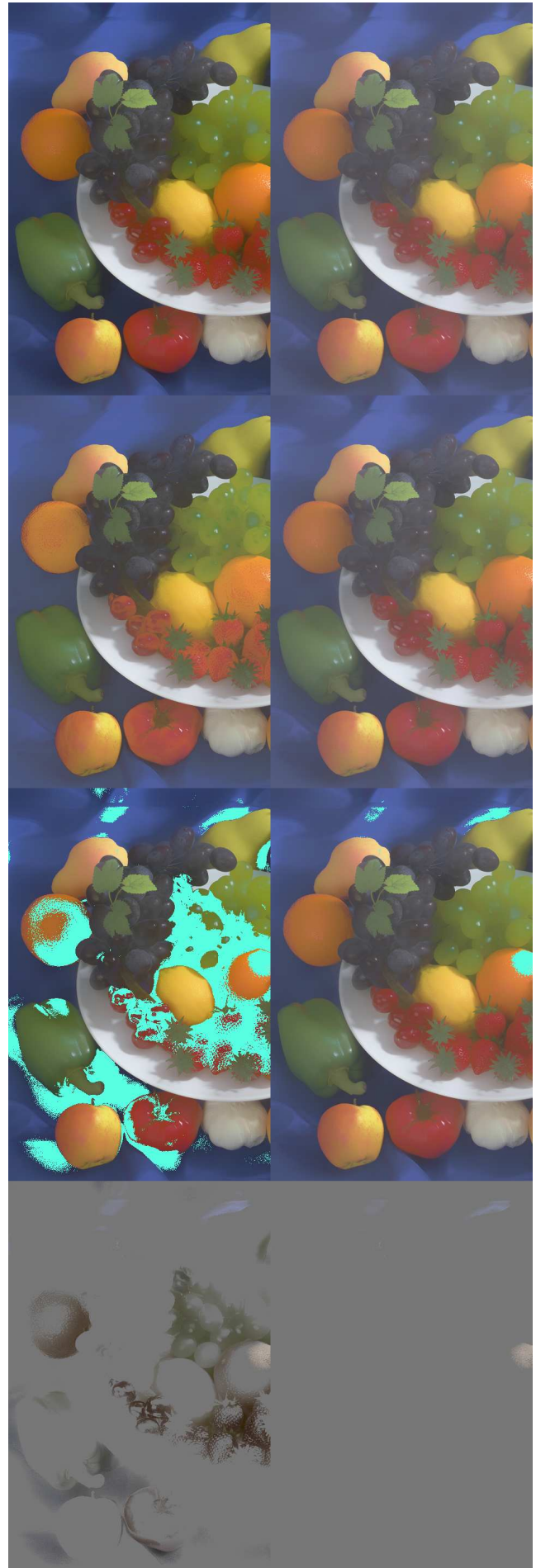


Figure 4. Impact of black point compensation.

Improvements in SCAGMAs

In this section we propose a set of improvements of SCACLIP and SCACOMP. First an adaptive merging of I_{low} and I_{high} is proposed, then modified projection in SCACOMP and modified energy minimization in SCACLIP are presented.

Adaptive merging of I_{low} and I_{high}

In first version of the SCAGMAs, I_{low} is mapped then I_{high} is added to I_{low} . When image areas of I_{low} have been greatly modified by the clipping, the newly composed image might have strong local distortions. Areas in the image where both I_{low} and I_{high} have large energies but I_{low} has lost most of its energy, it might be wise to reduce the energy in I_{high} to maintain a balanced ratio between contributions from both bands. Therefore we introduce $\alpha(i, I_{low}, I_{high})$ a local variable affecting the amount of I_{high} being added to I_{low} during the merging at each pixel i .

$$I_n = f_n(I_{low} + \alpha \cdot I_{high}), n \in \{1, 2, 3\}, \quad (8)$$

$$\alpha^i = \min\left(\sum_{j \in I_n} w_{BF}^j \frac{\|p_{low}^j - p_{low}^i\| + C1}{\|p_{low}^j - p_{low}^i\| + C1}, 1\right), \quad (9)$$

where $C1$ is a small constant value and w_{BF}^j are the weights of the bilateral filter used in the decomposition of the image (see Eq. 1). In our experiments we set $C1 = 0.001$ with p_{low} and p_{low} normalized in range $[0, 1]$. α is taken into account in the modified versions of SCACOMP (see Eq. 10) and SCACLIP (see Eq. 14).

Notice that α is less critical when Black Point Compensation is applied to I_{low} as the local structure of the low-pass band is then better preserved and α is often close to 1.

Modified projection in SCACOMP

SCACOMP, while being validated by psycho-physical experiments, can be further optimized by modifying the mathematical expression. In SCACOMP, each neighbor j contributes to the shifting of pixel i , weighted by w_{BF}^j defined by BF (see Eq. 1). In this evolution of SCACOMP, each neighbor's contribution is controlled by w_{shift}^i :

$$p_{out}^i = SCLIP(p_{low}^i + \alpha^i p_{high}^i) + w_{shift}^i p_u^i, \quad (10)$$

where p_u^i is the unit vector toward 50% grey,

$$w_{shift}^i = \sum_{j \in I_n} w_{BF}^j \max(p_{offset}^j \cdot p_u^i - |p_{offset}^j|, 0), \quad (11)$$

$$p_{offset}^j = SCLIP(p_{low}^j + \alpha^j p_{high}^j) - (p_{low}^j + \alpha^j p_{high}^j), \quad (12)$$

and where “ \bullet ” denotes the scalar product (see Fig. 5).

As $w_{shift}^i \geq 0$, the resulting color value lies in the gamut, between the gamut boundary and the 50% greypoint of $Gamut_{Dest}$. This modification prevents numerical imprecisions which could arise with very small values of $|p_{offset}^j|$.

Modified energy minimization in SCACLIP

In SCACLIP, to maintain the content of I_{high} the direction of the projection has been set as a variable: for each pixel the optimal mapping direction is chosen so that the local variations are best maintained. SCACLIP, while being validated by psycho-physical experiments, can be further optimized by changing the mathematical expression of the energy to preserve. To get faster results, the choice is restricted to a set of 3 directions proposed in published algorithms: $f_1 = HPMin\Delta E_a$, $f_2 = CUSP$ and $f_3 = SCLIP$ [1]. I_{high} and I_{low} are merged and the 3 mappings f_n , $n \in \{1, 2, 3\}$, are run:

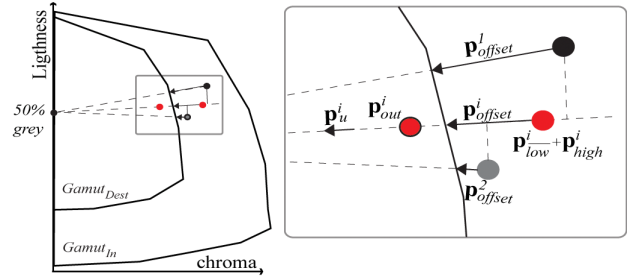


Figure 5. SCACOMP: p_{offset}^j ($j=1$) contributes to the shifting of $(p_{low}^i + p_{high}^i)$ toward the 50% greypoint, unlike p_{offset}^j ($j=2$).

$$I_n = f_n(I_{low} + \alpha^i I_{high}), n \in \{1, 2, 3\}. \quad (13)$$

In this new evolution of SCACLIP, the energy is defined as follows:

$$E_n^i = \sum_{j \in I_n} w_{BF}^j \| (p_{f_n}^j - p_{f_n}^i) - \alpha^i \cdot (p_{in}^j - p_{in}^i) \|. \quad (14)$$

Then the direction of projection for which E_n^i is the smallest is selected for the pixel i (see Fig. 6):

$$select = \arg \min_n (E_n^i), n \in \{1, 2, 3\}, \quad (15)$$

$$p_{out}^i = f_{select}(p_{low}^i + p_{high}^i). \quad (16)$$

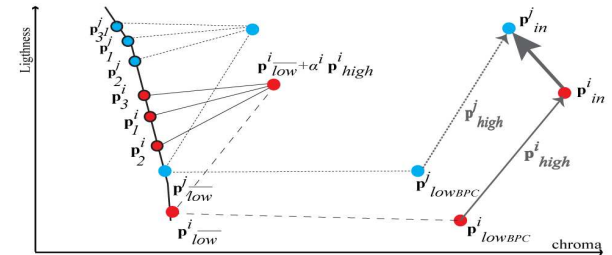


Figure 6. In modified SCACLIP the direction of projection of each pixel is selected to preserve as much as possible the vectors p_{in}^j .

The goal of this modification is better minimize the local differences between the original image and the resulting image.

Summary: Proposed Algorithms

The modified versions of SCACOMP and SCACLIP are described by the diagram in Fig. 7 and by the following process:

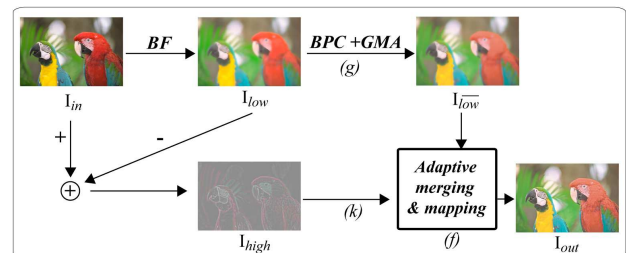


Figure 7. Framework for new Spatial and Color Adaptive Gamut Mapping.

1. Conversion of the original image to the CIELAB color space using the relative intent of the input ICC profile: I_{in} .

2. Decomposition in two bands using bilateral filtering (BF) [13]: I_{low} and I_{high} .
3. Black Point Compensation [17] of I_{low} : I_{lowBPC} .
4. $HPMin\Delta E$ clipping [14] of I_{lowBPC} : I_{low} .
5. Adaptive merging of I_{low} and I_{high} .
6. Adaptive mapping: I_{out}
7. Conversion to the CMYK encoding of the output printer using the relative colorimetric intent of its ICC profile.

Conclusions

A set of modifications has been introduced to improve results of two previous spatial and color adaptive gamut mapping algorithms: change in the image decomposition, an initial Black Point Compensation (BPC) algorithm of the low-pass band followed by an adaptive merging of the two bands. With these modifications, significant improvements have been obtained on images previously subject to artifacts (see Fig. 8). Black point compensation solves most of previous drawbacks and lessens the differences between results obtained with SCACOMP and SCA-CLIP.

More studies are needed to achieve optimal image decomposition: adaptive black point compensation will be investigated, we also need to better understand why results on prints are not as convincing as the one on monitor.



Figure 8. Comparison of mapping algorithms to the gamut of an Océ Colorwave 600 printer with standard paper. Top: original SCID-LAB image from ISO 12640-3. Second: BPC on original followed by $HPMin\Delta E$. Third: previous SCACLIP. Bottom: modified SCACLIP.

References

- [1] J. Morovic and R. Luo, "The fundamentals of gamut mapping: A survey," *The Journal of Imaging Science and Technology*, no. 3 ISBN / ISSN: 1062-370, vol. 45, pp. 283–290, 2001.
- [2] J. J. McCann, "Color gamut mapping using spatial comparisons," in *Proc. SPIE, Color Imaging*, VI, vol. 4300, pp. 126–130, 2001.
- [3] P.-L. Sun, *The Influence of Image Characteristics on Colour Gamut Mapping*. Derby, UK: University of Derby PhD Thesis, 2002.
- [4] R. Kimmel, D. Shaked, M. Elad, and I. Sobel, "Space dependent color gamut mapping: A variational approach," in *Proceedings of IEEE Transactions on image processing*, pp. 796–803, 2005.
- [5] J. Meyer and B. Barth, "Color gamut matching for hard copy," *SID 89 Digest*, 1989.
- [6] J. M. Kasson, *Color Image Gamut-Mapping System with Chroma Enhancement at Human-Insensitive Spatial Frequencies*. US Patent 5,450,216, 1995.
- [7] S. Nakauchi, S. Hatanaka, and S. Usui, "Color gamut mapping based on a perceptual image difference measure," in *Color Research and Application*, vol. 24, pp. 280–290, 1999.
- [8] R. Balasubramanian, R. deQueiroz, and R. Eschbach, "Gamut mapping to preserve spatial luminance variations," in *Eighth Color Imaging Conference: Color Science and Engineering Systems, Technologies, Applications*, ISBN / ISSN: 0-89208-231-3, vol. 1, (Scottsdale, Arizona), pp. 122–128, 2000.
- [9] J. Morovic and Y. Wang, "A multi-resolution, full-colour spatial gamut mapping algorithm," in *11th IS&T/SID Color Imaging Conference*, pp. 282–287, 2003.
- [10] P. Zolliker and K. Simon, "Adding local contrast to global gamut mapping algorithms," in *Third European Conference on Colour in Graphics, Imaging, and Vision (CGIV)*, vol. 1, pp. 257–261, 2006.
- [11] I. Farup, C. Gatta, and A. Rizzi, "A multiscale framework for spatial gamut mapping," in *IEEE Transactions on Image Processing*, No. 10, October 07, vol. 16, pp. 2423–2435, 2007.
- [12] N. Bonnier, F. Schmitt, M. Hull, and C. Leynadier, "Spatial and color adaptive gamut mapping: A mathematical framework and two new algorithms," in *To appear in Proceedings of the 15th IS&T/SID Color Imaging Conference*, vol. 1, (Albuquerque, NM), 2007.
- [13] C. Tomasi and R. Manduchi, "Bilateral filtering for gray and color images," in *ICCV '98: Proceedings of the Sixth International Conference on Computer Vision*, (Washington, DC, USA), p. 839, IEEE Computer Society, 1998.
- [14] CIE TC 8-03, *Guidelines for the evaluation of Gamut Mapping Algorithms*. CIE, 2004.
- [15] J. Morovic, *To Develop a Universal Gamut Mapping Algorithm*. Derby, UK: University of Derby, PhD Thesis, 1998.
- [16] E. H. Adelson, E. P. Simoncelli, and W. T. Freeman, "Pyramids and multiscale representations," in *Proc European Conf on Visual Perception*, (Paris), August 1990.
- [17] L. Borg and Adobe Systems, "Adobe systems implementation of black point compensation," in [http : //www.color.org/AdobeBPC.pdf](http://www.color.org/AdobeBPC.pdf) , downloaded 08/2007, 2002.
- [18] J. Holm, "Some considerations in the development of color rendering and gamut mapping algorithms," vol. 5678, pp. 137–143, SPIE, 2005.
- [19] G. Braun and M. Fairchild, "Image lightness rescaling using sigmoidal contrast enhancement functions," in *Proc. IS&T-SPIE Electronic Imaging Color Imaging Device Independent Color Color Hardcopy and Graphic Arts IV*, (San Jose, CA), pp. 96–105, 1999.
- [20] P. Green, *Gamut mapping and appearance models in graphic arts colour management*. Derby, UK: University of Derby, PhD Thesis, 2003.
- [21] International Color Consortium, "ICC.1:2004-10," in [http : //www.color.org/icc_specs2.html](http://www.color.org/icc_specs2.html) , downloaded 03/2006, 2004.
- [22] F. Durand and J. Dorsey, "Fast bilateral filtering for the display of high-dynamic-range images," in *SIGGRAPH '02: Proceedings of the 29th annual conference on Computer graphics and interactive techniques*, (New York, NY, USA), pp. 257–266, ACM Press, 2002.

Author Biography

Nicolas Bonnier graduated from ENS Louis Lumière (Paris) in 2000, major in photography, and received his Master degree in Electronic Imaging from Université Pierre et Marie Curie (Paris) in 2001. He was a member of the Laboratory for Computational Vision with Pr Simoncelli at the New York University from 2002 to 2005. Then he started a PhD program in 2005 under the direction of Pr Schmitt, TELECOM ParisTech, sponsored by Océ. He is now a color scientist with Océ whom he represents in the International Color Consortium.